Research Article

Maik Rahlves*, Christian Kelb, Eduard Reithmeier and Bernhard Roth

Methodology for the design, production, and test of plastic optical displacement sensors

DOI 10.1515/aot-2016-0027
Received April 19, 2016; accepted May 31, 2016; previously published online June 25, 2016

Abstract: Optical displacement sensors made entirely from plastic materials offer various advantages such as biocompatibility and high flexibility compared to their commonly used electrical and glass-based counterparts. In addition, various low-cost and large-scale fabrication techniques can potentially be utilized for their fabrication. In this work we present a toolkit for the design, production, and test of such sensors. Using the introduced methods, we demonstrate the development of a simple all-optical displacement sensor based on multimode plastic waveguides. The system consists of polymethylmethacrylate and cyclic olefin polymer which serve as cladding and core materials, respectively. We discuss several numerical models which are useful for the design and simulation of the displacement sensors as well as two manufacturing methods capable of mass-producing such devices. Prior to fabrication, the sensor layout and performance are evaluated by means of a self-implemented ray-optical simulation which can be extended to various other types of sensor concepts. Furthermore, we discuss optical and mechanical test procedures as well as a high-precision tensile testing machine especially suited for the characterization of the opto-mechanical performance of such plastic optical displacement sensors.

Keywords: displacement measurement; hot embossing; integrated plastic optics; lamination techniques; plastic optics; polymer sensors.

***Corresponding author: Maik Rahlves,** Hannover Centre for Optical Technologies, Nienburger Straße 17, 30167 Hannover, Germany, e-mail: maik.rahlves@hot.uni-hannover.de
Christian Kelb and Bernhard Roth: Hannover Centre for Optical Technologies, Nienburger Straße 17, 30167 Hannover, Germany
Eduard Reithmeier: Hannover Centre for Optical Technologies, Nienburger Straße 17, 30167 Hannover, Germany; and Institute of Measurement and Automatic Control, Nienburger Straße 17, 30167 Hannover, Germany

1 Introduction

Displacement and strain sensors are employed in a large variety of applications ranging from structural health monitoring (SHM) over mechanical analysis of prototypes to biomedical applications [1, 2]. From an industrial point of view, fabrication and material costs are important aspects with regard to mass production of such devices. While the majority of commercially available sensing devices are based on electrical strain gauges, usually manufactured by lithographical techniques, optical strain sensors based on glass-optical fibers are also commercially available. These offer advanced multiplexing potential through the large number of sensor units which can be integrated at relatively low cabling complexity. Although a large number of different purely plastic-made sensor concepts have already been demonstrated, only a few are commercialized, and research on strain or displacement measurement using fiber Bragg gratings (FBG) or optical frequency domain reflectometry is still vital.

In general, the design of plastic optical sensors is highly specific to their particular field of application and is most often based on polymer optical fibers (POF) or other types of polymer-optical waveguides. For strain, displacement, and temperature measurement, FBG sensors are prominent examples as they provide a high sensitivity for detection of environmental influences such as moisture. The physical principle relies on a periodic refractive index modification, which is usually created by transferring a grating pattern into the core of a POF by means of UV laser writing. The grating serves as a Bragg filter and reflects a distinct wavelength at the Bragg wavelength of the grating from a broadband light spectrum being transmitted through the POF. Thermal or mechanical loads induce a change of the Bragg wavelength, and, thus, a shift of the reflected wavelength can be detected by spectroscopic means. Typical applications of FBGs include displacement and strain measurement in SHM or wavelength selective filters in telecommunication, among others. Also, a

micro-structured dual core POF was reported to selectively capture antibodies with a sensitivity of 20.3 nm per nanometer thickness of the biolayer [3]. Alternative methods to optically measure strain, deflection, or temperature include interferometric sensors. For instance, a membrane attached to the end of a fiber or waveguide serves as Fabry-Perot resonator, where the cavity length changes due to mechanical or thermal loads or water absorption [4]. Other fiber-based sensors to measure force and pressure include POF fibers which are embedded inside a wavelike structure to induce microbends [5, 6]. Applying force to the sensor changes light leakage out of the POF and, thus, changes the transmitted intensity. Intensity modulation can also be achieved by creating a recess between two opposing fibers sharing the same optical axis. A relative displacement of both fibers then leads to a change in the transmitted intensity. Such fully plastic-made sensors were demonstrated for displacement and strain measurements [7]. A comprehensive study on various plastic optic displacement sensors is given in [8]. Typical values for the sensitivity and linear measurement interval are in the range from 0.0001 mV/μm to 1.7615 mV/mm and 46 μm to 2000 μm, respectively. However, the total performance of such sensors strongly depends on ambient light as well as humidity and temperatures especially when using polymethylmethacrylate (PMMA) based fibers. Polymers such as cyclic olefin polymers offer a promising alternative to PMMA enabling strain measurements at temperatures as high as 110°C [9, 10]. For the fabrication of such integrated optical devices, various fabrication methods ranging from hot embossing, micro-injection molding [11], and lithographic methods to laser direct writing [12] can be utilized. The selection of a suitable fabrication process is, in general, based on the required feature sizes, throughput rates, and polymer material of the sensor [13].

In this paper we discuss a general methodology for the development of simple plastic optical displacement sensors. The methodology comprises a rough estimation of the sensor performance based on the available materials and production processes, an adapted method for the optical simulation of given waveguide structures, and optical as well as mechanical test procedures. Also, a short overview over useful numerical methods for the simulation as well as hot embossing and lamination as two suitable production processes is given. We discuss modeling of the displacement sensor and the production thereof, and we present measurement results with regard to mechanical stability, waveguide attenuation, and optical performance.

2 Optical design concepts for displacement sensors

In this section, we give a brief overview of algorithms for the simulation of light propagation which forms the basis for the design of our plastic optical sensor systems. We then give a detailed example of the layout and optical design of a fully plastic-made optical displacement sensor, with particular emphasis on multimode optical waveguides.

2.1 Simulation methods

The major aim when performing optical design tasks is to optimize the optical layout of a sensor system and, thus, the sensing performance with respect to a given measurement application and range. In general, optical sensors are designed by means of algorithms which trace light through an optical system consisting of various discrete elements. A suitable selection of an adequate physical model forms the basis of efficient simulation algorithms utilized for the design task and depends on the geometrical dimension of the integrated optical elements, i.e. the dimension of the cross section of the waveguide core as well as the refractive indices of the core and cladding region. If feature sizes of the optical elements are in the lower micron or even submicron range, wave-optical algorithms are required for optical modeling and simulation purposes [14]. Existing methods commonly used are not necessarily specific to plastic optics but are also utilized in silicon photonics. For instance, optical gratings can be designed using rigorous coupled-wave analysis (RCWA), where it is assumed that the electromagnetic field propagates in certain diffraction orders as defined by the grating [15]. However, RCWA approaches are limited to periodical structures such as the above gratings. Alternatively, finite-difference or finite-element methods are frequently used [16]. While the first methods are restricted to simulation volumes of a few ten cubic microns, the latter may be utilized to describe light propagation as well as mechanical and thermal changes of the sensor, which is of special interest in plastic optics. Both have in common that the simulation region is discretized by a simulation grid and Maxwell or Helmholtz equations are solved. Typical applications of both methods are the design of sensors operated in the single-mode regime such as ring resonators which can also be utilized to realize polymer displacement sensors [17]. If waveguide dimensions increase and more than one mode is guided, commonly used design methods include both

eigenmode expansion and also the well-known beam-propagation method (BPM). Using the latter method, it is assumed that the electrical field in propagation direction, i.e. along the optical axis of a waveguide, is only slowly varying. As a consequence, the initial implementation of the BPM is limited to straight waveguides, but numerical extensions to curved structures were introduced and are now available in commercial design tools such as RSoft™ or Optiwave™.

If dimensions of cross sections further increase to the multimode regime, the above simulation methods are not suitable due to a high numerical effort and convergence problems. Therefore, classical raytracing methods are utilized as optical design tool. In this work, we focus exemplarily on a displacement sensor with a single emitter-detector pair. As reported in [7], an array of several emitter-detector pairs can be used to also detect tilt simultaneously. The physical principle of the sensor is based on multimode waveguides with cross sections of 100 µm, and, thus, raytracing is the most suitable design approach. While in classical raytracing approaches an imaging system is designed by optimizing the shape of optically relevant surfaces and the arrangement of lenses as well as other optical elements, in certain cases such as for the fiber-based sensor presented here the intensity distribution behind an optical fiber is of special interest.

Intensity distributions can be simulated by means of classical Monte Carlo-based methods where a large number of rays are traced through the optical system starting from the light source. However, this method usually requires a vast amount of computational effort. Therefore, using the ray-tracing method proposed by Bescherer et al. in [18] is better suited for our application. The method traces rays from a given region in front of the waveguide to its output facet taking into account the coupling conditions given by the waveguide's numerical aperture (NA) and front facet geometry. The algorithm yields an intensity map behind the waveguide and can also take, e.g. non-Lambertian intensity distributions inside the waveguide into account. It greatly decreases computational effort for the calculation of the intensity distribution for a broad parameter space. The calculated resulting intensity map behind a flat-facet 100 µm embedded waveguide is shown in Figure 1A. Light intensity transmitted through such a waveguide and detected at its output facet is the quantity used to optically detect and quantify environmental effects acting on the system, for example, displacement, temperature, or humidity. The change of intensity can then be used for the estimation of the sensor sensitivity which can be achieved. Furthermore, the numerical simulation data in combination with measured data from manufactured sensors can be employed for sensor optimization. This is exemplified in Figure 1B which shows a differently shaped waveguide facet profile obtained with a confocal microscope scan. In this simulation, the profile is approximated with a flat front and circular edges with a diameter of 5 µm. The simulations were carried out using a wavelength of 578 nm, which corresponds to the yellow line of a mercury lamp. Note that the refractive index depends on the wavelength and was assumed to be 1.53. In our own work, we already demonstrated the feasibility of this approach for modeling and simulation of optical strain sensors utilizing flat and lensed waveguides [19].

2.2 Design of plastic optical displacement sensors

The way to an integrated optical sensor system requires evaluating a certain number of different design concepts as exemplified in this work for the case of a simple displacement sensor. The sensor is based on two optical waveguides in a butt-coupling arrangement, with one waveguide being the emitter and one waveguide being the receiver, shown in Figure 2 for different waveguide

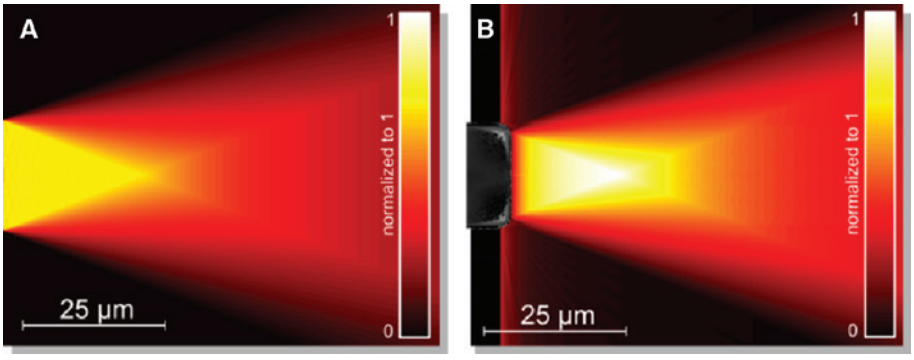

Figure 1: Simulated intensity distributions behind the end facet of a multimode optical fiber: (A) Planar end facet, (B) curved end facet.

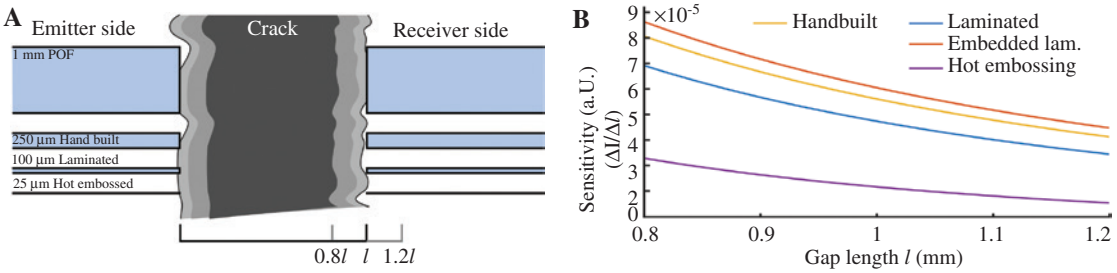

Figure 2: (A) Schematic of butt-coupling type displacement sensors of different dimensions attached to a crack to be monitored, (B) simulated sensitivity $\Delta I/\Delta l$ (change in coupled intensity I over change in gap width l) for the different sensor concepts and production technologies.

structure sizes, as available from different production methods. In this configuration, the optical intensity coupled between emitter and receiver waveguide is solely depending on the gap length l. As sketched in Figure 2A, the emitter-receiver pair can be mounted on a, e.g. building wall across a crack, monitoring the change in gap length as the crack widens or narrows over time. We will stick to this scenario to demonstrate application of the suggested methodology.

Depending on the intended use of the displacement sensor, e.g. for monitoring of cracks in building structures or as strain sensors in wearables equipped with optical functionality, different requirements with regard to sensitivity, ruggedness, or unit price are to be met. These can be accounted for by choosing an appropriate production technology such as hot embossing or lamination. The particular choice, however, influences other properties of the sensor system since, e.g. hot embossing is more capable of creating very small waveguide structures in the sub-micron range, while lamination is restricted to linear or mostly linear waveguide designs but offers a higher throughput rate and greatly reduced tooling costs. For the continuous monitoring of a hypothetically 1 mm wide crack on a building wall, important requirements on the design of such a sensor are the achievable sensitivity within the defined measurement range of 1 mm in this case and a certain ruggedness against varying thermal loads or humidity. Figure 2B shows the theoretically achievable sensitivity over the given measurement range for manually assembled, laminated, and hot embossed waveguide structures as basic building blocks of the displacement sensor. The theoretical values were obtained by a rough geometrical estimation of the coupling efficiency for a displacement scenario assuming a circular waveguide cross section.

Since absorption of environmental moisture and water droplets or street dust on the waveguides front facets would influence the measurement result, either the sensor has to be enclosed in a water- and airtight case or the fibers have to be embedded in a flexible substrate, both shielding the sensor from environmental influences. Given its high chemical resistance, long-term stability, and low cost, polydimethylsiloxane (PDMS), a silicon-based polymer material that also displays excellent optical quality, can serve as a shielding material. The sensor sensitivity for the PDMS-embedded laminated waveguides changes compared to the non-embedded waveguides. In our case, the resulting sensitivity (red curve in Figure 2B) increases over the whole displacement range due to the smaller waveguide NA in the PDMS substrate compared to air. Also, even in this rough estimation, it can be observed that the embedding of the sensor in PDMS increases the sensitivity above the level of the 'hand-built' sensor (yellow curve) that exhibits twice the structure size.

2.3 Production and processing methods

Large-scale fabrication of plastic optical sensors imposes high demands with regard to reproducibility and reliability, throughput rates, and material costs. Especially, roll-to-roll capable processes such as lamination or hot embossing can fulfill these demands. Here, we discuss the main aspects of both processes used and focus on the fabrication of waveguide-based displacement sensors by lamination.

2.3.1 Hot embossing

In hot embossing, a pattern is transferred into a thermosoftening plastic substrate such as PMMA by heating a mold and the plastic substrate above its glass transition temperature [13]. An embossing force is subsequently applied for a defined embossing time, followed by a cooling and release process step. Common mold materials include

silicon, copper, or nickel, which are either directly microstructured by lithographic processes or diamond tooling or formed by electroplating [13, 20]. The hot embossing device itself can be set up either in a plate-to-plate configuration where a plane substrate holder and a plane mold are utilized (see Figure 3A) or, alternatively, in a roll-to-roll process as shown in Figure 3B. If a plate-to-plate configuration is utilized, a common tool size is 4″ as often 4″ microstructured silica wafers are used as mold. The dimension of the optical structures is generally in the 25 µm range but can reach down to sub-micron range, e.g. optical gratings. For the roll-to-roll process, a micro-patterned roller drum serves as mold, and a second roller acts as counterpart to achieve the embossing force as shown in Figure 3. To heat the substrate and mold, various concepts were realized including infrared heaters, see Figure 3, or direct heating of the roller drums [21]. Since hot embossing is a fast process to structure surfaces of thermoplastics, it has been utilized to create micro-structures in applications ranging from diffractive optics [20] and holograms as security labels to lab-on-chip sensors for bioanalytical purposes [13].

However, for waveguide fabrication, two different materials with different refractive indices serving as core and cladding materials are required which cannot be processed by a single hot embossing process directly. Therefore, an initial hot embossing step is often used to pattern the cladding material, which yields trenches in a thermoplastic substrate. In a next process step, a liquid core material in a monomer state is often deposited onto the substrate to fill the trenches [22]. To distribute the core material on the substrate, various methods are utilized including a doctor blading process [23] or covering the bottom substrate containing the trenches with a second additional cladding layer on top [22, 24]. In both cases, a residual layer on top of the substrate consisting of the core material remains and needs to be sufficiently thin to avoid stray light propagating inside the cladding and crosstalk between adjacent waveguides. Using both processes, the fabrication of low-loss waveguides has been demonstrated [22, 24]. Polymerization of the core material is either initiated by UV radiation or by thermal heat depending on the specific type of core material used [22]. An example of a hot embossed polymer waveguide structure consisting of five emitter-detector pairs for combined displacement and tilt measurement is shown in Figure 3C. The sensor design also contains two continuous waveguides for testing purposes.

2.3.2 Lamination

If the layout of an optical system to be created is sufficiently simple, roll-to-roll lamination is an adequate fabrication technique for mass production of such devices. For instance, the sensor presented in this work to demonstrate the fabrication methodology can be realized by lamination of a single core filament between two substrate layers (Figure 4A). Recently, we reported a roll-to-roll lamination process that enables the production of mechanically stable multi-layer structures containing embedded waveguides by using cyclic olefin polymer (COP) filament and PMMA cladding with reproducible optical quality suitable for low-loss wave guiding.

Since COP and PMMA are immiscible, lamination of both materials is not feasible without further preparation of the polymers. Using an active lamination agent based on PMMA containing photoreactive 2-acryloyloxy-anthraquinone units that is spray-coated onto the COP filaments beforehand, Rother et al. recently demonstrated the lamination of both materials [25]. Utilizing the same materials and lamination agent, we were able to obtain roll-to-roll suitable production of embedded waveguides based on a hot-roll laminator.

While the process features very high throughput rates and can easily be upscaled, it can only be applied

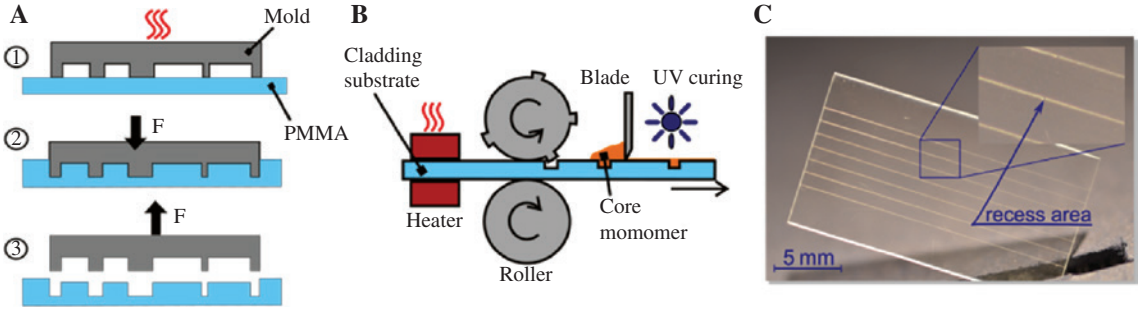

Figure 3: (A) Hot embossing process in plate-to-plate configuration consisting of heating (1), applying an embossing force F (2), and demolding (3), (B) waveguide fabrication based on roll-to-roll hot embossing, (C) hot embossed sensor prototype; the position of linear recesses between opposing waveguides is indicated in the enlargement.

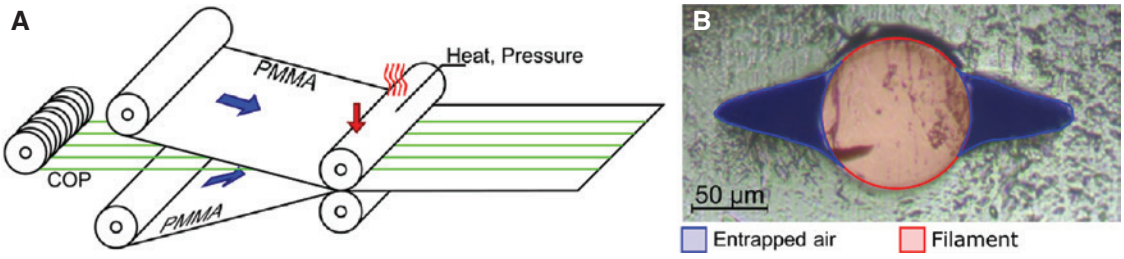

Figure 4: (A) Roll-to-roll lamination process for five parallel COP waveguides in a PMMA substrate, (B) profile of the embedded filament with entrapped air on the left and right.

to manufacture straight or slightly bent waveguides (e.g. by guiding the waveguide with a moving nozzle). Also, air inclusions close to the filament and the bond area between upper and lower cladding are characteristic features of the process (Figure 4B). These inclusions are generated by laminating the planar PMMA substrates around the circular cross-section filament. The size of the air inclusions can be decreased by increasing the lamination temperature inside the substrate which is achieved by increasing the roll temperature or decreasing the lamination speed, thus allowing more time for heat being conducted from the lamination rolls to the center of the laminated stack. However, the resulting increase in core temperature of the stack may result in a slight deformation of the waveguide core if the lamination temperature approaches the glass transition temperature of the filament. If carried out with a single filament, the process yields an endless one-waveguide 'ribbon cable' that can be separated into single-substrate chips. Two of such chips, placed 1 mm apart and connected to optical fibers on the outer ends, yield the already simulated simple displacement sensor.

2.4 Sensor characterization and performance

The characterization of the manufactured systems can encompass several different steps, depending on the utilized production technology. The involved tests can be divided into geometrical tests (measuring the dimensional accuracy and shape deviation), mechanical tests (measuring e.g. the performance of the system under mechanical stress) and optical tests (measuring attenuation or beam propagation in the system).

2.4.1 Optical characterization

Since the sensor, as most proposed integrated optical systems, features embedded waveguides, the most prominent method to evaluate the performance of such optical structures is the attenuation measurement. To date, a variety of methods to approach this task have been demonstrated, among others, scattering light detection [26] or techniques using the waveguide as a Fabry-Perot cavity [27]. The most important one, however, is the cutback method or variations thereof [28]. It is carried out by coupling light into a waveguide of length l and measuring the output intensity I either by using end-facet coupling or by monitoring the output facet with a beam profiler. By successively shortening the waveguide and repeating the measurement, the method yields a set of measurement points of intensity over length that follows an exponential increase with decreasing waveguide length (Figure 5A). However, the waveguide itself is destroyed during the measurement. The measurement setup utilized for attenuation measurements is shown in Figure 5B. It consists of a fiber coupled LED light source (M625F1, Thorlabs™) with a center wavelength of 625 nm which is attached to a multimode fiber with a core diameter of 50 µm used for launching light into the sample waveguide. The light intensity being transmitted through the waveguide is measured by a beam profiler (620U, Ophir Spiricon™) with a 20× microscope lens (Plan N, Olympus™).

To ensure accurate and reliable measurement results using this method, careful end facet preparation and reproducible coupling conditions are main requirements. The attenuation value is obtained from the decay parameter of the exponential fit, which cannot, however, account for discontinuities in the measured data. Therefore, the waveguide has to be as homogenous as possible throughout its entire length. Depending on the production process, discontinuities are caused by small air inclusions or dust particles if the system is processed from liquid resin, by surface defects for laser-written waveguides, or by filament cracks, bends, and again dust particles in the case of a laminated system. These defects result in a steeper slope of the exponential fit and an inaccurate (too large) estimate of the attenuation value. A decrease in coupled intensity on the other hand is observed, if the surface quality of the

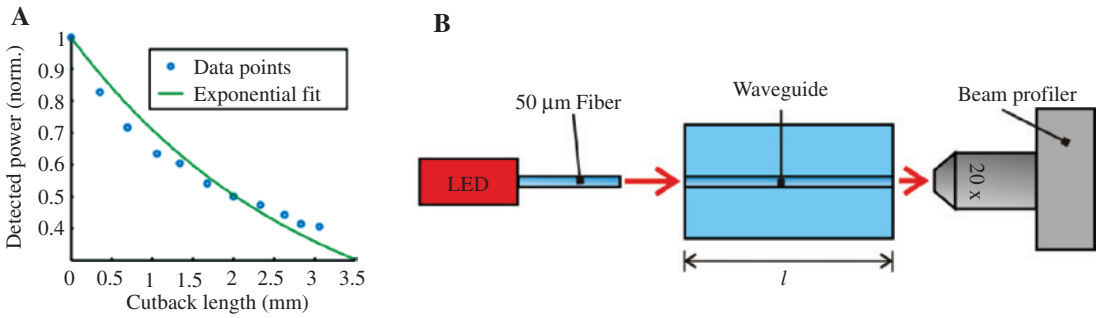

Figure 5: (A) Experimental results of the attenuation measurement of a laminated waveguide using the cutback method, (B) experimental setup for attenuation measurements.

end facets deteriorates with each successive cutback step. As these steps are often carried out using a hot blade in case of polymer systems, wear of the blade over several cuts may cause an increasing number of scratch marks on the output facet. These scratch marks decrease the power being measured by the beam profiler and, thus, the slope of the measured intensity values. While waveguide defects can easily be avoided by optical inspection and pre-selection of waveguides, scratch marks can only be avoided by ensuring stable waveguide preparation and coupling conditions for each cutback step. The described method was carried out exemplarily for waveguides fabricated through the described lamination method. Typical attenuation values for such laminated waveguides are in the range of 1.4 dB/cm, which were obtained utilizing an incoherent light source at a center wavelength of 625 nm. For hot embossed waveguides structures, typical attenuation values are in the range of 0.8 dB/cm, measured using a diode laser with a center wavelength of 638 nm.

2.4.2 Mechanical characterization

To test if the produced sensor system meets the performance criteria, further tests need to be carried out. With the described simple sensor system, two main requirements have to be met: Light propagation inside the device needs to be sufficiently close to the simulation results, and the mechanical link between the materials used, in this case COP filament and PMMA substrate, has to be durable. Both specifications can be evaluated utilizing a high-precision tensile testing device such as the one illustrated in Figures 6 and 7A.

For the device, we chose a horizontal design which allows placement of the sample under study on an optical table for combined optical and opto-mechanical tests either in free space or in fiber coupled configuration. It features two sledges, both supported on air bearings. While one sledge is connected to a force sensor (AST KAP-S/2 kN), the other sledge is connected to a stepper motor (Nanotec ST5909L3008-B) with a drive screw. The choice to use the rather expensive air bearings over conventional linear ball bearings allows the measurement of very small forces without interference by breakaway forces within the laminated samples.

To determine the mechanical stability of the sensor system, a so-called pull-out test can be performed where a filament located between two laminated substrate layers is pulled out and the applied force is measured. In the best case, the filament will break without being pulled out, which indicates a stable chemical bond between waveguide material and substrate material. This is in particular advantageous for polymer-based sensors operated in harsh environments in order to ensure longevity and

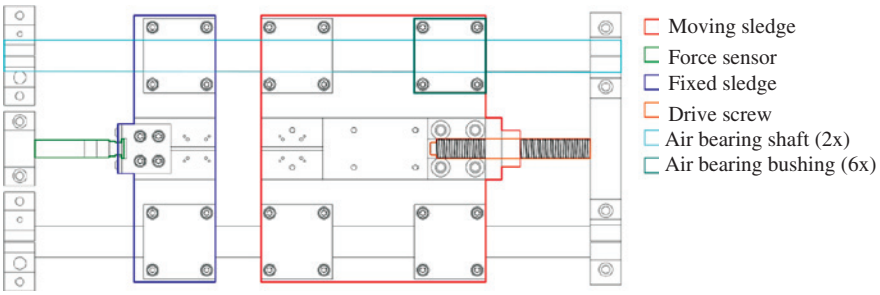

Figure 6: Schematic of the developed high-precision tensile testing machine. Different sub-assemblies are marked with different colors.

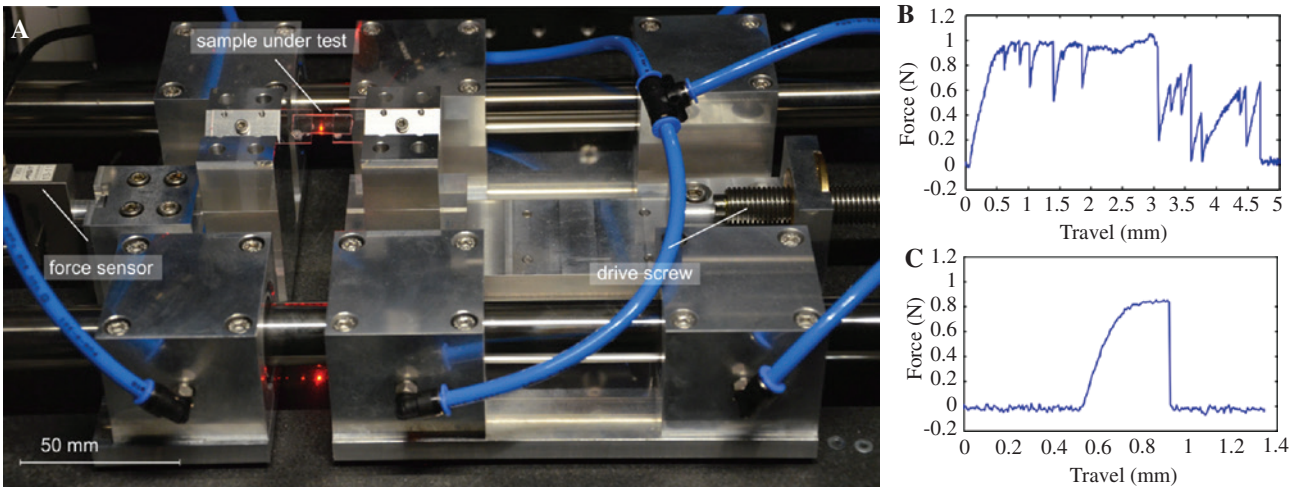

Figure 7: (A) Photograph of the tensile testing machine, here with a grating under test, with laser light coupled in free-space configuration, (B) force-over-travel curve of a failed pull-out test, exhibiting a sawtooth pattern from alternating slipping and sticking of the laminated filament, (C) force-over-travel curve of a successful pullout test.

reliable sensor operation and to prevent delamination. A failed pull-out test will be indicated by a sawtooth like force-over-travel curve as shown in Figure 7B, caused by the slip-stick between core filament and substrate layers, while the filament is pulled out. The result of a successful pullout test is shown in Figure 7C. Here, as the travel was increased the filament tore at a maximum force, indicating a durable chemical bond between both materials. Note that the spikes in the measurement which are observable in Figure 7B indicate a failure in adhesion between core and cladding material and are not due to faulty measurement.

With a maximum force of 2 kN, even comparably stiff sensor arrays can be characterized, which is crucial for sensors in SHM where the monitored relative movements are mostly slow but at high amplitude. The minimum force which can still be detected is 0.1 N (with a signal-to-noise ratio of 1 dB) allowing a test of very flexible sensors that are needed when specimen motion is not supposed to affect the sensor performance.

2.4.3 Sensor performance

The performance of the sensor with regard to displacement measurement was evaluated utilizing the setup shown in Figure 8B. For launching light into the sensor and measuring the output power, the same setup was utilized as for the attenuation measurements shown in Figure 5B. While the emitter side of the sensor was fixated, the receiver chip was moved over a distance ranging from l=0 mm to 1.5 mm in increments of approximately 100 µm using a

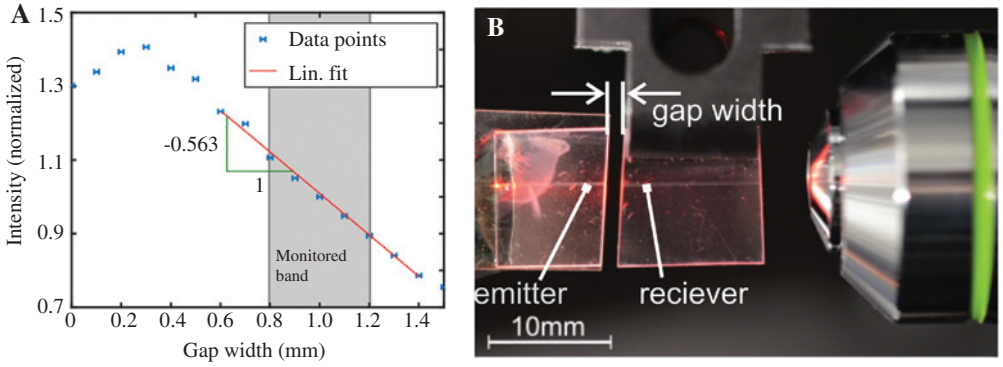

Figure 8: (A) Coupled power from the emitter to the receiver waveguide of the produced sensor, normalized to 1 for a gap width of 1 mm, (B) setup for the performance test, using one part of the laminated waveguide as emitter (left), the other part as a receiver (right) and monitoring the output facet of the receiver with a beam profiler (only the microscope lens in front of the beam profiler is shown on the outer right).

three-axis mechanical translation stage (Saidev™), thus emulating a change in the gap width l. The transmitted power was measured by an Ophir SP620U beam profiler at the output facet of the receiver chip as a function of the gap width and is shown in Figure 5B. The intensity was normalized at a gap width of l=1 mm. The slope of a linear fit to the intensity value yields a sensitivity for displacement measurement of the sensor of -0.56 mm^{-1}. The result is comparable to the ones obtained by raytracing simulations (compare Figure 2B) presented above, which yielded sensitivity values of -0.34 mm^{-1}. The higher sensitivity may be caused by the NA of the laminated waveguide, which varies due to air inclusions, as shown in Figure 4B.

Note that PMMA is prone to water absorption which leads to geometrical deformations of the sensor and may introduce a significant measurement error. The same effect is commonly caused by a variation of the ambient temperature leading to a total cross-sensitivity between displacement and ambient conditions such as humidity and temperature. Both can be accounted for by including a second identical reference sensor with its measurement direction being perpendicular to the displacement measurement direction. The second sensor measures the influence of the ambient conditions on the sensor response which is then used to correct the response of the first sensor to yield accurate displacement measurement values. These effects and correction procedures were not in the focus of the current study but will be part of future studies including climate camber experiments with alternating temperature and humidity.

3 Summary and discussion

In this work we discussed a methodology for the design, fabrication, and optical as well as mechanical characterization of fully plastic-made sensor systems. We focused in particular on simple planar displacement sensors designed for monitoring cracks in building walls, for example. For the optical sensor design, several commonly used numerical models to describe light propagation in plastic optical systems were briefly revised with a special emphasis on ray-optical models suitable for efficient modeling and simulation. These were used to design the displacement sensor based on multimode optical waveguides. The concept relies on a linear recess across one or several adjacent multimode waveguides. The recess defines an elongation zone, whose length varies as a function of displacement. As the length of the elongation zone is altered, the coupling efficiency between the two opposite waveguides changes which can be directly related to the displacement to be measured. In addition to optical design aspects of such sensor systems, we discussed hot embossing and lamination as two roll-to-roll capable processes for large-scale and low-cost fabrication of such sensors and present the results achieved.

The fabricated systems are characterized with regard to waveguide losses, mechanical stability, and optical performance. We presented and describe the test methods used with special emphasis on possible sources of error. We also presented an in-house built tensile testing machine for precise mechanical and opto-mechanical tests, explaining the benefits of the proposed design especially regarding sensor characterization. With the results from loss measurements obtained on laminated waveguides, data from pull-out tests, and the performance of the produced displacement sensors for gap widths of 0–1.5 mm, we could demonstrate the overall functionality of the concept and, thus, prove the validity of the proposed methodology. In future work, the presented toolbox for design, fabrication, and opto-mechanical characterization will be extended to different and more complex displacement and force sensor designs potentially reaching high sensitivity and paving the way for low-cost and large-scale fabrication of such devices with possible applications in process monitoring and SHM or the life sciences.

Acknowledgments: This work was funded by the German Research Foundation (DFG) in the framework of the collaborative research center TRR 123-PlanOS. We are grateful to Maher Rezem who provided the hot embossed waveguide samples.

References

[1] C. I. Merzbacher, A. D. Kersey and E. J. Friebele, Smart. Mater. Struct. 5, 196–208 (1996).
[2] P. Roriz, O. Frazão, A. B. Lobo-Ribeiro, J. L. Santos and J. A. Simões, J. Biomed. Opt. 18, 50903 (2013).
[3] C. Markos, W. Yuan, K. Vlachos, G. E. Town and O. Bang, Opt. Express 19, 7790–7798 (2011).
[4] F. J. Arregui, Y. Liu, I. R. Matias and R. O. Claus, Sensor. Actuat. B-Chem. 59, 54–59 (1999).
[5] Z. Chen, J. T. Teo, S. H. Ng and X. Yang, IEEE Sensors. 1–4 (2012).
[6] M. Linec and D. Donlagic, IEEE Sensors J. 7, 1262–1267 (2007).
[7] C. Kelb, M. Rahlves, E. Reithmeier and B. Roth, IEEE Sensors J. 15, 7029–7035 (2015).
[8] H. Z. Yang, X. G. Qiao, D. Luo, K. S. Lim, W. Y. Chong, et al., Measurement 48, 333–345 (2014).
[9] C. Markos, S. Stefani, K. Nielsen, H. K. Rasmussen, W. Yuan, et al., Opt. Express 21, 4758–4765 (2013).
[10] G. Woyessa, A. Fasano, A. Stefani, C. Markos, K. Nielsen, et al., Opt. Express 24, 1253–1260 (2016).

[11] F. Dortu, D. Bernier, I. Cestier, D. Vandormael, C. Emmerechts, et al., in '16th International Conference on Transparent Optical Networks – ICTON (2014)', 1–4.2 (IEEE, Piscataway, NJ, USA).
[12] W. M. Pätzold, C. Reinhardt, A. Demircan and U. Morgner, Opt. Lett. 41, 1269–1272 (2016).
[13] M. Worgull, Hot Embossing, (William Andrew Publishing, Boston, MA, 2009).
[14] B. E. A. Saleh and M. C. Teich, Fundamentals of Photonics, 2nd ed. (Wiley-Interscience, Hoboken, N.J., 2007).
[15] M. G. Moharam, T. K. Gaylord, E. B. Grann and D. A. Pommet, J. Opt. Soc. Am. A 12, 1068 (1995).
[16] A. Bondeson, T. Rylander and P. Ingelström, Computational Electromagnetics, 2nd ed. (Springer, New York, London, 2012).
[17] J. N. Fields, C. K. Asawa, O. G. Ramer and M. K. Barnoski, IEEE Photon. Technol. Lett. 17, 867–869 (2005).
[18] K. Bescherer, D. Munzke, O. Reich and H.-P. Loock, Appl. Optics 52, B40–B45 (2013).
[19] C. Kelb, E. Reithmeier and B. Roth, Proc. SPIE 8977, 89770Y (2014).
[20] M. Rahlves, M. Rezem, K. Boroz, S. Schlangen, E. Reithmeier, et al., Opt. Express 23, 3614 (2015).
[21] T. Velten, H. Schuck, W. Haberer and F. Bauerfeld, Int. J. Adv. Manuf. Technol. 47, 73–80 (2010).
[22] M. Rezem, A. Günther, M. Rahlves, B. Roth and E. Reithmeier, Procedia Technol. 15, 514–520 (2014).
[23] M. Rezem, C. Kelb, A. Günther, M. Rahlves, E. Reithmeier, et al., Proc. SPIE 9751, 975112 (2016).
[24] H. Mizuno, O. Sugihara, T. Kaino, N. Okamoto and M. Hosino, Opt. Lett. 28, 2378 (2003).
[25] R. Rother, A.-K. Schuler, C. Müller, O. Prucker, J. Rühe, et al., Proc. SPIE 9627, 96270I (2015).
[26] K. Gut and K. Nowak, Eur. Phys. J. Spec. Top. 154, 89–92 (2008).
[27] T. Feuchter and C. Thirstrup, IEEE Photon. Technol. Lett. 6, 1244–1247 (1994).
[28] A. Boudrioua and J. Loulergue, New approach for loss measurements in optical planar waveguides, Opt. Commun. 137, 37–40 (1997).